ACS Photonics

pubs.acs.org/journal/apchd5 Article

Demonstration of N-Polar III-Nitride Tunnel Junction LED

Yuantao Zhang,* Gaoqiang Deng, Ye Yu, Yang Wang, Degang Zhao, Zhifeng Shi, Baolin Zhang, and Xiaohang Li*

Cite This: ACS Photonics 2020, 7, 1723–1728

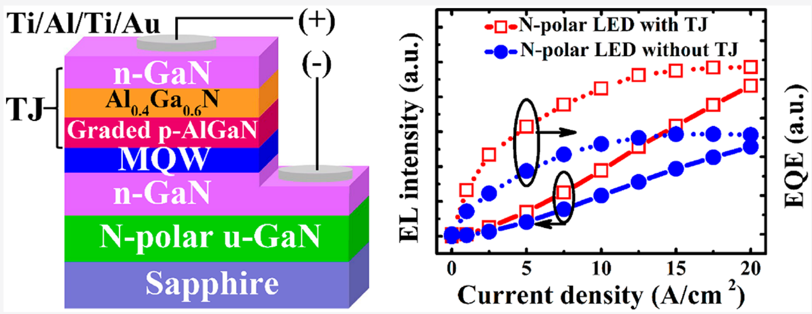

ABSTRACT: In this study, we have demonstrated an N-polar III-nitride tunnel junction (TJ) light-emitting diode (LED). The LED was grown on an N-polar GaN template on sapphire substrates by metal-organic vapor phase epitaxy. The growth started with the n-GaN cladding layer, whose doping condition was optimized by the periodic doping method, and then the InGaN/GaN quantum well active region. Subsequently, the TJ was grown comprising a graded p-AlGaN layer, a thin undoped $Al_{0.4}Ga_{0.6}N$ interlayer, and the topmost n-GaN layer. The *I*−*V* measurement shows that the device resistance of the TJ LED was significantly reduced compared to the reference LED without the TJ due to enhanced hole injection. The electroluminescence measurement manifested that the emission and the external quantum efficiency of the TJ LED were greatly enhanced by ∼70% compared with the reference LED. This work demonstrates that the TJ devices can be realized amid the N-polarity that is promising for high-performance devices operating at various wavelengths.

KEYWORDS: *N-polar, tunnel junction, light-emitting diodes, UV, visible*

With an adjustable direct band gap, III-nitride semiconductor materials have been widely employed for technically important visible and UV optoelectronics such as light-emitting diodes (LEDs) and laser diodes (LDs).[1−5] For light-emitting devices, the electron-supplying n-(Al)GaN layer and the hole-supplying Mg-doped p-(Al)GaN layer are indispensable. The n-GaN with a high electron concentration above 10^{18} cm^{-3} can be achieved by Si- or Ge-doping and can be as high as 2.9×10^{20} cm^{-3}.[6,7] However, the hole concentration in optimized p-GaN is commonly low (<10^{18} cm^{-3}) due to a high activation energy of ∼200 meV for acceptors.[8] The activation energy increases monotonically in p-AlGaN with higher Al content, resulting in even lower hole concentration.[9,10] The low hole concentration leads to high resistivity, low hole injection efficiency, and poor lateral current spreading,[11,12] which are some of the main factors limiting the optoelectronic device performance.[13] In the past, efforts have been made to increase the hole concentration of p-(Al)GaN. The Mg-doping concentration of GaN epilayers can reach up to 5×10^{19} cm^{-3}, resulting in a free hole concentration of 5.5×10^{17} cm^{-3}.[14−17] Recently, Simon et al. demonstrated a hole concentration of 10^{18} cm^{-3} by the polarization doping technique in a compositionally graded AlGaN:Mg layer.[18] Also, it has been reported that the device resistance can be significantly reduced by the use of a tunnel junction (TJ) because it enhances the hole injection and eliminates the need of the p-type cladding layer with relatively low hole concentration.[19,20] Therefore, we expect that the combination of the polarization doping and the TJ could bring about overall improved device performance thanks to higher hole concentration and better lateral current spreading.

It is noted that most of the reported III-nitride TJs have been based on the III-polarity. Recently, some excellent works on N-polar GaN/InGaN/GaN TJs have been reported to be grown by metal-organic vapor phase epitaxy (MOVPE) and molecular beam epitaxy (MBE). Krishnamoorthy et al.

Received: February 20, 2020
Published: May 28, 2020

https://dx.doi.org/10.1021/acsphotonics.0c00269
ACS Photonics 2020, 7, 1723–1728

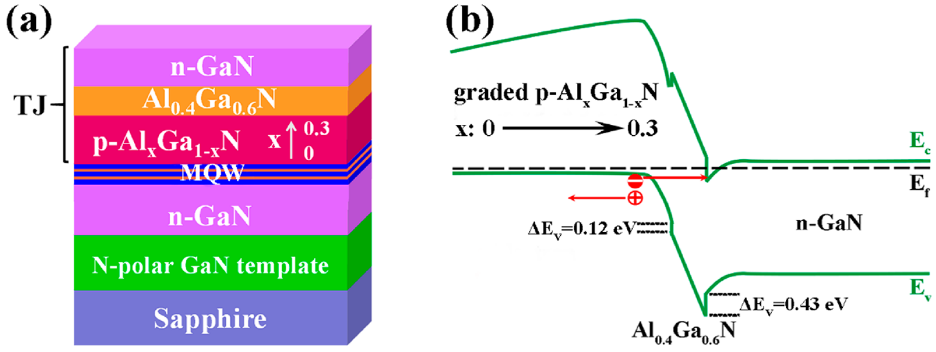

Figure 1. (a) Cross-sectional schematic diagram of the N-polar TJ LED wafer. (b) Schematic energy band diagram of the TJ.

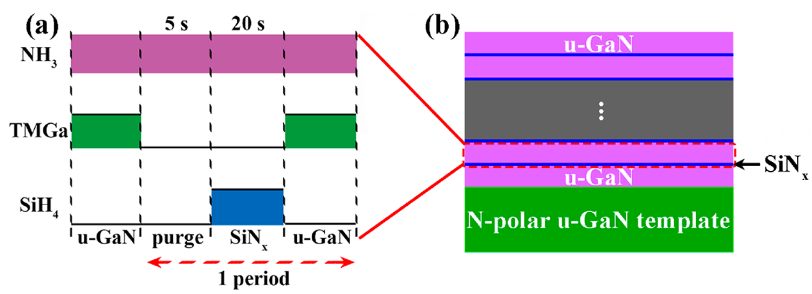

Figure 2. (a) Source on/off sequencing of the SiH_4 delta doping method for Series II and III and (b) cross-sectional schematics of the n-GaN layer by the periodic SiH_4 delta doping method. The purging time and the SiH_4 flow time are 5 and 20 s, respectively. The one-period thickness in Series II is 20 nm for four samples with SiH_4 flow rates of 2, 10, 16, and 20 nmol/min. The one-period thicknesses in Series III are 10, 15, and 20 nm for three samples by increasing the u-GaN thickness of one period with the same SiH_4 flow rate of 10 nmol/min.

demonstrated an N-polar p-GaN/$In_{0.33}Ga_{0.67}N$/n-GaN TJ.[21] Yan et al. reported the realization of an N-polar p-GaN/$In_{0.25}Ga_{0.75}N$/n-GaN Zener TJ.[22] Lund et al. demonstrated an N-polar p-GaN/$In_{0.35}Ga_{0.65}N$/n-GaN TJ by MOVPE.[23] Despite this progress, N-polar TJ LEDs have not been demonstrated to our knowledge, which has essentially limited the applications of N-polar TJs. This is in stark contrast to the III-polar counterparts, where the III-polar TJ LEDs have already been reported by various groups.[24−26]

In this work, we have demonstrated an N-polar TJ LED. This is achieved (1) by optimizing the growth process of the N-polar n-GaN layer and (2) by employing the polarization doping technique for the p-type layer of the TJ. The EL intensity of the N-polar TJ LED is significantly higher that of the reference N-polar LED without the TJ.

Shown in Figure 1(a), the TJ comprises a 75-nm-thick graded p-$Al_xGa_{1-x}N$ ($x = 0$−0.3) layer, a 5-nm-thick undoped $Al_{0.4}Ga_{0.6}N$, and a 150-nm-thick n-GaN top contact layer. The schematic energy band diagram of the TJ is shown in Figure 1(b). The band gap of $Al_xGa_{1-x}N$ is obtained according to the formula[27] $E_{g,AlxGa_{1-x}} = xE_{g,AlN} + (1 - x)E_{g,GaN} + bx(1 - x)$, where $E_{g,AlxGa_{1-x}N}$, $E_{g,AlN}$, and $E_{g,GaN}$ are the band gaps of $Al_xGa_{1-x}N$, AlN, and GaN, respectively, and b is the bowing parameter. $E_{g,GaN}$ = 3.4 eV, $E_{g,AlN}$ = 6.2 eV, and b = 1 are adopted for the calculation.[28] The band offset ratio of $\Delta E_c/\Delta E_v$ = 0.5:0.5 is used for the GaN/AlGaN heterostructure.[29] The calculated ΔE_v between GaN and $Al_{0.4}Ga_{0.6}N$ is ~0.43 eV, and that between $Al_{0.4}Ga_{0.6}N$ and $Al_{0.3}Ga_{0.7}N$ is ~0.12 eV. As shown in Figure 1(b), the electrons in the valence band of the p-graded AlGaN layer could transport to the conduction band of the n-GaN by tunneling when the reverse bias is applied to the TJ. As a result, the holes are generated in the valence band of the p-graded AlGaN layer to inject into the active region, thereby enhancing the hole injection as opposed to having the dedicated p-cladding layer and the p-contact for hole injection.

EXPERIMENTAL METHODS

The entire epitaxial structures were grown by an MOVPE system using common group-III precursors and NH_3. Bis-cyclopentadienyl magnesium (Cp_2Mg) and silane (SiH_4) were utilized as p- and n-type dopants, respectively. First, the 2-μm-thick N-polar unintentionally doped GaN (u-GaN) templates were deposited on *c*-plane sapphire substrates.[30] Subsequently, a 500-nm-thick n-GaN cladding layer was grown, followed by the five-period InGaN (3 nm)/GaN (14 nm) multiple-quantum-well (MQW) active region and then the TJ, all of which inherited the N-polarity from the u-GaN template. The growth temperatures of the InGaN quantum well (QW) layer and GaN quantum barrier (QB) are 775 and 950 °C, respectively. Both QW and QB layers are unintentionally doped. Unlike the growth of III-polar n-GaN layers nowadays, the growth condition of the N-polar n-GaN layer was not trivial, because the Si doping condition could have a profound impact on the surface morphology and doping profile, which are important to the subsequent active region and the TJ. However, few studies have been reported to optimize the doping condition of the N-polar n-GaN layer. Since N-polar n-GaN is employed as the n-type cladding layer and part of the TJ, it is important to optimize its epitaxial conditions. We have carried out three series (I, II, III) of growth experiments with different SiH_4 doping schemes on the N-polar u-GaN templates. The layer thickness, surface temperature, and V/III ratio were kept at 500 nm, 1080 °C, and 1500 for the n-GaN layers of the three series.

https://dx.doi.org/10.1021/acsphotonics.0c00269
ACS Photonics 2020, 7, 1723−1728

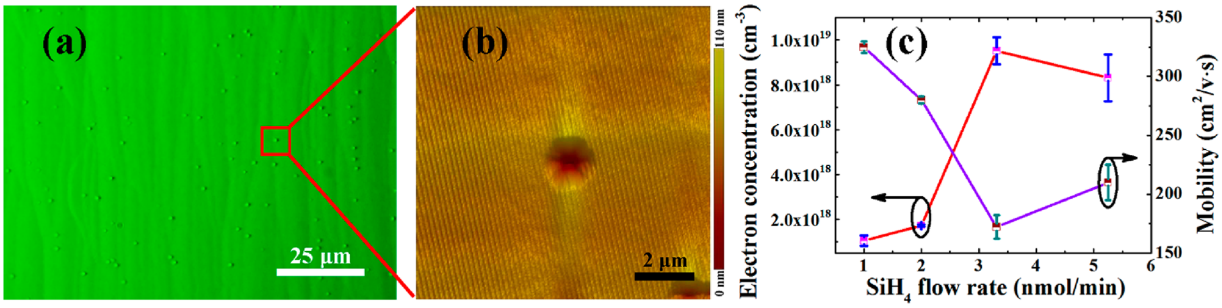

Figure 3. (a) OM image of the typical sample surface in Series I, where this image is from the sample with the SiH_4 flow rate of 3.4 nmol/min. (b) AFM image of the area marked by the red square in (a). (c) Dependence of the electron concentration and the mobility on the SiH_4 flow rate for the N-polar n-GaN samples in Series I.

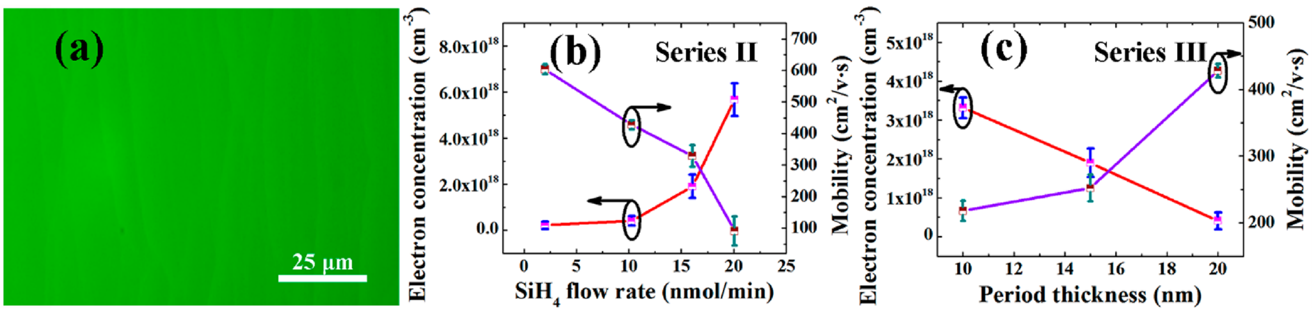

Figure 4. (a) Typical OM image of typical surface morphology of the N-polar n-GaN samples in Series II and III, where this image is from the sample with the SiH_4 flow rate of 16 nmol/min. The electron concentration and the mobility as a function of (b) SiH_4 flow rate (Series II) and (c) period thickness of the delta-doped layer (Series III).

In Series I, four n-GaN layers were grown at four different SiH_4 flow rates of 1, 2, 3.4, and 5.4 nmol/min while keeping SiH_4, TMGa, and NH_3 on continuously.

In Series II, four n-GaN layers were grown using the periodic delta doping method shown in Figure 2, where SiH_4 and TMGa were alternatively switched on and off while NH_3 was kept on continuously. At the beginning of each period, there was a 5 s purging time where neither SiH_4 nor TMGa was flown into the reactor. Previously, the SiH_4 delta doping method has been applied to the III-polar n-GaN growth but not yet for the N-polar n-GaN growth.[31−33] Thus, the n-GaN layers in Series II essentially comprise the periodic superlattice comprising unintentionally doped u-GaN and SiN_x layers. Each period corresponded to a 20 nm thickness for Series II. The four samples in Series II were grown using various SiH_4 flow rates of 2, 10, 16, and 20 nmol/min to investigate the influence of the SiH_4 flow rates.

For the three n-GaN samples in Series III, the growth utilized the same delta doping method as Series II. But the period thickness of the delta-doped layer varied, 10, 15, and 20 nm, by changing the growth time of the u-GaN layer with a constant SiH_4 flow rate of 10 nmol/min to study the impact of the period thickness. Basically, the thickness of the SiN_x layers was the same in Series II and III. What changed in Series III is the thickness of the u-GaN layers. The surface morphology of the samples of Series I, II, and III was examined by optical microscopy (OM) and atomic force microscopy (AFM). The electron concentrations were measured by Hall at room temperature (RT).

■ RESULTS AND DISCUSSION

The OM measurement shows that the typical surface of the samples in Series I exhibits a dot-like morphology, as shown in Figure 3(a). Besides, the surface undulation can be observed in Figure 3(a), which results from the step-bunching growth mode.[34] The AFM image in Figure 3(b) shows that the dot-like morphology in Figure 3(a) is actually a hexagonal V-pit. The V-pits can act as paths of current leakage that deteriorate device performance.[35] Figure 3(c) shows that the electron concentration and the mobility of the Series I samples vary with the SiH_4 flow rate. The electron concentrations increase slowly when the SiH_4 flow rate rises from 1 to 2 nmol/min and rapidly as the SiH_4 flow rate elevates to 3 nmol/min. Meanwhile, the further increase of the SiH_4 flow rate leads to a decrease of the electron concentration, which may be related to the self-compensation effect.[36] The above measurement results show that the electron concentration and the mobility in the N-polar n-GaN layers do not possess proportionality with the SiH_4 flow rate and thereby cannot be well controlled using the conventional continuous growth method, in addition to the surface pit issue.

Figure 4(a) shows a typical OM image of the n-GaN sample surface in Series II and III, where the dot-like morphology is not found, indicating elimination of the V-pits by using the periodic Si-delta-doping method. Figure 4(b) illustrates the electron concentration and the mobility of the Series II samples as a function of the SiH_4 flow rate. We find that the electron concentration shows a superlinear increase with the SiH_4 flow rate, even when the SiH_4 flow rates are much higher than the one used for Series I. For Series III, the electron concentration manifests a linear reduction with increased period thickness of the delta-doped layers, as shown in Figure 4(c).

Through the comparison of the measurement results for the samples in Series I−III, the periodic Si-delta-doping method can not only suppress the formation of V-pits but also realize

https://dx.doi.org/10.1021/acsphotonics.0c00269
ACS Photonics 2020, 7, 1723−1728

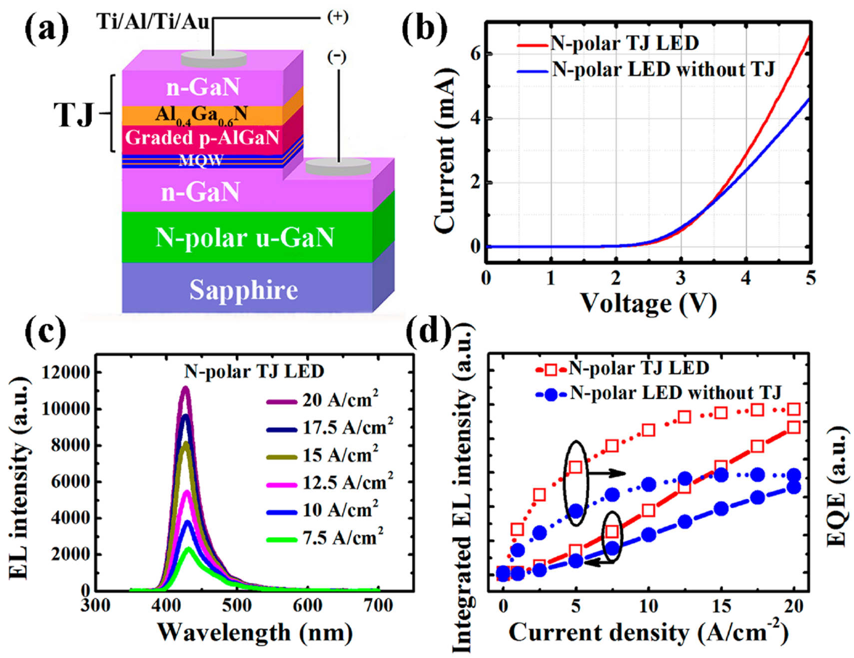

Figure 5. (a) Schematic diagram of the TJ LED under EL operation. (b) $I-V$ curves of the TJ LEDs and the reference LED. (c) EL spectra of the TJ LED under a current density ranging from 7.5 to 20 A/cm^2. (d) Integrated EL intensity and relative EQE of the TJ LED and the reference LED as a function of current density.

highly controllable and predictable electron concentration in the N-polar n-GaN. Also, we can infer that the formation of the V-pits is closely related to the doped Si atoms in N-polar n-GaN. We speculate that the suppressed formation of V-pits may be related to the reduced tensile stress amid the periodic Si-delta doping as compared to the conventional continuous Si doping in N-polar GaN.[37−40] It is worth noting that the n-GaN cladding layer in the proposed TJ LED structure was prepared using the periodic Si-delta-doping method, for which the period thickness of the delta-doped layers and the SiH_4 flow rate were 20 and 16 nmol/min, respectively. The corresponding n-GaN layer had a relatively high electron mobility of 329 ± 34 cm^2/V·s and electron concentration of ∼(2.0 ± 0.5) × 10^{18} cm^{-3}, shown in Figure 4(b).

With the optimized N-polar n-GaN cladding layer grown on the u-GaN template, the rest of the TJ LED structure was grown by MOVPE comprising the MQW active region and the TJ. The growth conditions of the active region and the graded p-$Al_xGa_{1-x}N$ layer were the same as those in our previous N-polar LED report.[41] It is noted that to achieve high hole concentration by the polarization doping method, the graded layer should not be too thick because the volumetric concentration of polarization charges is inversely proportional to the grading distance.[42] Thus, the commonly reported thickness of the graded layer has been small, i.e., 50−80 nm, which was adopted in this study (i.e., 75 nm).[18,41,43] The hole concentration and mobility of the graded p-$Al_xGa_{1-x}N$ layer were 9 × 10^{17} cm^{-3} and 7.5 cm^2/V·s at RT, respectively. Additionally, a reference N-polar LED wafer was grown and fabricated for devices. It has the same structure as the TJ LED except that the TJ is replaced by the 75-nm-thick graded p-$Al_xGa_{1-x}N$ (x = 0−0.3) layer, which is covered by a 3 nm p+-$Al_{0.3}Ga_{0.7}N$ contact layer. The growth conditions of the MQW region in the reference LED are the same as those in the TJ LED.

The LED mesa structures with an area of 250 μm × 250 μm were fabricated with an inductively coupled plasma (ICP) etching system. The $I-V$ characteristics and top-emitting EL spectra of the N-polar TJ LED and the N-polar reference LED were measured. Figure 5(a) shows the schematic diagram of the TJ LED. Owing to the existence of the TJ, the cathode and anode to n-GaN can be obtained at one time with the Ti/Al/Ti/Au metal stack. For the reference LED, the cathode and anode are Ti/Al/Ti/Au and Ni/Au metal stacks, respectively. Other than the metal stack composition, the TJ LED and the reference LED share the same electrode layout for a fair EL comparison.

Figure 5(b) shows the $I-V$ curves of the TJ LED and the reference LED. Both LEDs have a turn-on voltage of ∼2.5 V. The total resistance of the TJ LED (264 Ω) is significantly (40%) lower than that of the reference LED (439 Ω) from the linear regime (4−5 V) of the $I-V$ curves. Figure 5(c) shows the EL spectra of the TJ LED under different current densities with the EL peak at ∼430 nm, and the reference LED emits at the same wavelength. As exhibited in Figure 5(d), the integrated EL intensities of the two LEDs increase monotonically with current density. It is noted that the integrated EL intensity of the TJ LED becomes higher than that of the reference LED above 2 A/cm^2, and the disparity increases amid larger current density. At 20 A/cm^2, the EL intensity of the TJ LED is 70% higher than that of the reference LED, a significant enhancement. Figure 5(d) also manifests the relative external quantum efficiency (EQE) as a function of the current density by dividing the integrated EL intensity by the injection current.[44] It can be seen that the EQE of the TJ LED is significantly higher than that of the reference LED. At 20 A/cm^2, for instance, the EQE of the TJ LED is 1.7 times that of the reference LED, which is consistent with the EL enhancement. The significantly enhanced EL intensity and EQE are attributed to the lower total resistance resulting by the TJ. It is worth mentioning that the proposed TJ in this

https://dx.doi.org/10.1021/acsphotonics.0c00269
ACS Photonics 2020, 7, 1723−1728

work can be applied to other spectral ranges, not only UVB and UVC, but also longer wavelength yellow and red with modifications of material and structural parameters. Also it is noted that the current density of the TJ in this work is still lower than those of the reported N-polar GaN/InGaN/GaN TJs, which may be caused by the use of Al-rich AlGaN for the TJ, though it could be improved by further optimization.

CONCLUSIONS

In summary, we have demonstrated the N-polar III-nitride TJ LED grown by MOVPE on the sapphire substrate. The TJ comprises the N-polar n-GaN/$Al_{0.4}Ga_{0.6}N$/graded p-$Al_xGa_{1-x}N$ double heterojunction. The doping condition of n-GaN was thoroughly optimized by the periodic Si-delta-doping method to suppress the formation of the V-pits and realize good control of the electron concentration and the mobility. Thanks to the improved hole injection, the device resistance of the TJ LED is ~40% lower than that of the reference LED without the TJ. Consequently, the EL intensity and the EQE of the TJ LED are 70% higher than those of the reference LED at $20 A/cm^2$. This study manifests great potentials of the TJ to be employed in N-polar devices. Moreover, although the TJ LED emits at visible wavelengths, the proposed TJ can be applied to other spectral ranges such as UVC, UVB, yellow, and red by further optimization.

AUTHOR INFORMATION

Corresponding Authors

Yuantao Zhang − *State Key Laboratory of Integrated Optoelectronics, College of Electronic Science and Engineering, Jilin University, Changchun 130012, China;* orcid.org/0000-0002-8671-6979; Phone: +86-431-85168241(8261); Email: zhangyt@jlu.edu.cn

Xiaohang Li − *Advanced Semiconductor Laboratory, King Abdullah University of Science and Technology (KAUST), Thuwal 2395-6900, Saudi Arabia;* orcid.org/0000-0002-4434-365X; Phone: +966-128087335; Email: xiaohang.li@kaust.edu.sa

Authors

Gaoqiang Deng − *State Key Laboratory of Integrated Optoelectronics, College of Electronic Science and Engineering, Jilin University, Changchun 130012, China*

Ye Yu − *State Key Laboratory of Integrated Optoelectronics, College of Electronic Science and Engineering, Jilin University, Changchun 130012, China*

Yang Wang − *State Key Laboratory of Integrated Optoelectronics, College of Electronic Science and Engineering, Jilin University, Changchun 130012, China*

Degang Zhao − *State Key Laboratory of Integrated Optoelectronics, Institute of Semiconductors, Chinese Academy of Science, Beijing 100083, China*

Zhifeng Shi − *Key Laboratory of Materials Physics of Ministry of Education, School of Physics and Microelectronics, Zhengzhou University, Zhengzhou 450052, China;* orcid.org/0000-0002-9416-3948

Baolin Zhang − *State Key Laboratory of Integrated Optoelectronics, College of Electronic Science and Engineering, Jilin University, Changchun 130012, China*

Complete contact information is available at: https://pubs.acs.org/10.1021/acsphotonics.0c00269

Notes

The authors declare no competing financial interest.

ACKNOWLEDGMENTS

This work was supported by the National Key Research and Development Program (no. 2016YFB0401801) and the National Natural Science Foundation of China (nos. 61674068, and 61734001). X.L. acknowledges the support of KAUST Baseline Fund BAS/1/1664-01-01, GCC Research Council Grant REP/1/3189-01-01, and Competitive Research Grants URF/1/3437-01-01 and URF/1/3771-01-01.

REFERENCES

(1) Ruterana, S.; Albrecht, M.; Neugebauer, J. *Nitride Semiconductors*, 1st ed.; Wiley-VCH, Weinheim, 2003; p 4.

(2) Meng, X.; Wang, L.; Hao, Z. B.; Luo, Y.; Sun, C. Z.; Han, Y. J.; Xiong, B.; Wang, J.; Li, H. T. Study on efficiency droop in InGaN/GaN light-emitting diodes based on differential carrier lifetime analysis. *Appl. Phys. Lett.* **2016**, *108*, 013501.

(3) Deng, G. Q.; Zhang, Y. T.; Yu, Y.; Yan, L.; Li, P. C.; Han, X.; Chen, L.; Zhao, D. G.; Du, G. T. Significantly improved surface morphology of N-polar GaN film grown on SiC substrate by the optimization of V/III ratio. *Appl. Phys. Lett.* **2018**, *112*, 151607.

(4) Sun, X. J.; Li, D. B.; Song, H.; Chen, Y. R.; Jiang, H.; Miao, G. Q.; Li, Z. M. Short-wavelength light beam in situ monitoring growth of InGaN/GaN green LEDs by MOCVD. *Nanoscale Res. Lett.* **2012**, *7*, 282.

(5) Wen, P. Y.; Liu, J. P.; Zhang, S. M.; Zhang, L. Q.; Ikeda, M.; Li, D. Y.; Tian, A. Q.; Zhang, F.; Cheng, Y.; Zhou, W.; Yang, H. Asymmetrical quantum well degradation of InGaN/GaN blue laser diodes characterized by photoluminescence. *Appl. Phys. Lett.* **2017**, *111*, 212102.

(6) Richter, E.; Stoica, T.; Zeimer, U.; Netzel, C.; Weyers, M.; Tränkle, G. Si doping of GaN in hydride vapor-phase epitaxy. *J. Electron. Mater.* **2013**, *42*, 820.

(7) Fritze, S.; Dadgar, A.; Witte, H.; Bügler, M.; Rohrbeck, A.; Bläsing, J.; Hoffmann, A.; Krost, A. High Si and Ga n-type doping of GaN doping - Limits and impact on stress. *Appl. Phys. Lett.* **2012**, *100*, 122104.

(8) Lyons, J. L.; Alkauskas, A.; Janotti, A.; Van de Walle, C. G. First-principles theory of acceptors in nitride semiconductors. *Phys. Status Solidi B* **2015**, *252*, 900.

(9) Goepfert, I. D.; Schubert, E. F.; Osinsky, A.; Norris, P. E.; Faleev, N. N. Experimental and theoretical study of acceptor activation and transport properties in p-type Al_xGa_{1-x} N/GaN superlattices. *J. Appl. Phys.* **2000**, *88*, 2030.

(10) Katsuragawa, M.; Sota, S.; Komori, M.; Anbe, C.; Takeuchi, T.; Sakai, H.; Amano, H.; Akasaki, I. Thermal ionization energy of Si and Mg in AlGaN. *J. Cryst. Growth* **1998**, *189-190*, 528.

(11) Li, C. K.; Rosmeulen, M.; Simoen, E.; Wu, Y. R. Study on the Optimization for Current Spreading Effect of Lateral GaN/InGaN LEDs. *IEEE Trans. Electron Devices* **2014**, *61*, 511.

(12) Liang, F.; Zhao, D. G.; Jiang, D. S.; Liu, Z. X.; Zhu, J. J.; Chen, P.; Yang, J.; Liu, W.; Li, X.; Liu, S. T.; Xing, Y.; Zhang, L. Q.; Yang, H.; Long, H.; Li, M. Improvement of Ohmic contact to p-GaN by controlling the residual carbon concentration in p++-GaN layer. *J. Cryst. Growth* **2017**, *467*, 1.

(13) Martens, M.; Kuhn, C.; Ziffer, E.; Simoneit, T.; Kueller, V.; Rass, J.; Wernicke, T.; Einfeldt, S.; Weyers, M.; Kneissl, M. Low absorption loss p-AlGaN superlattice cladding layer for current-injection deep ultraviolet laser diodes. *Appl. Phys. Lett.* **2016**, *108*, 151108.

(14) Li, T.; Simbrunner, C.; Wegscheider, M.; Navarro-Quezada, A.; Quast, M.; Schmidegg, K.; Bonanni, A. GaN: δ-Mg grown by MOVPE: Structural properties and their effect on the electronic and optical behavior. *J. Cryst. Growth* **2008**, *310*, 13.

(15) Wang, H.; Liu, J.; Niu, N.; Shen, G.; Zhang, S. Enhanced performance of p-GaN by Mg δ doping. *J. Cryst. Growth* **2007**, *304*, 7.

(16) Sirkeli, V. P.; Yilmazoglu, O.; Al-Daffaie, S.; Opera, I.; Ong, D. S.; Küppers, F.; Hartnage, H. L. Efficiency enhancement of InGaN/GaN light-emitting diodes with pin-doped GaN quantum barrier. *J. Phys. D: Appl. Phys.* **2017**, *50*, 035108.
(17) Lieten, R. R.; Motsnyi, V.; Zhang, L.; Cheng, K.; Leys, M.; Degroote, S.; Buchowicz, G.; Dubon, O.; Borghs, G. Mg doping of GaN by molecular beam epitaxy. *J. Phys. D: Appl. Phys.* **2011**, *44*, 135406.
(18) Simon, J.; Protasenko, V.; Lian, C. X.; Xing, H. L.; Jena, D. Polarization-Induced Hole Doping in Wide-Band-Gap Uniaxial Semiconductor Heterostructures. *Science* **2010**, *327*, 60.
(19) Neugebauer, S.; Hoffmann, M. P.; Witte, H.; Bläsing, J.; Dadgar, A.; Strittmatter, A.; Niermann, T.; Narodovitch, M.; Lehmann, M. All metalorganic chemical vapor phase epitaxy of p/n-GaN tunnel junction for blue light emitting diode applications. *Appl. Phys. Lett.* **2017**, *110*, 102104.
(20) Krishnamoorthy, S.; Akyol, F.; Park, P. S.; Rajan, S. Low resistance GaN/InGaN/GaN tunnel junctions. *Appl. Phys. Lett.* **2013**, *102*, 113503.
(21) Krishnamoorthy, S.; Park, P. S.; Rajan, S. Demonstration of forward inter-band tunneling in GaN by polarization engineering. *Appl. Phys. Lett.* **2011**, *99*, 233504.
(22) Yan, X. D.; Li, W. J.; Islam, S. M.; Pourang, K.; Xing, H. L.; Fay, P.; Jena, D. Polarization-induced Zener tunnel diodes in GaN/InGaN/GaN heterojunctions. *Appl. Phys. Lett.* **2015**, *107*, 163504.
(23) Lund, C.; Romanczyk, B.; Catalano, M.; Wang, Q. X.; Li, W. J.; DiGiovanni, D.; Kim, M. J.; Fay, P.; Nakamura, S.; DenBaars, S. P.; Mishra, U. K.; Keller, S. Metal-organic chemical vapor deposition of high quality, high indium composition Npolar InGaN layers for tunnel devices. *J. Appl. Phys.* **2017**, *121*, 185707.
(24) Jeon, S. R.; Song, Y. H.; Jang, H. J.; Yang, G. M.; Hwang, S. W.; Son, S. J. Lateral current spreading in GaN-based light-emitting diodes utilizing tunnel contact junctions. *Appl. Phys. Lett.* **2001**, *78*, 3265.
(25) Alhassan, A. I.; Young, E. C.; Alyamani, A. Y.; Albadri, A.; Nakamura, S.; DenBaars, S. P.; Speck, J. S. Reduced-droop green III-nitride light-emitting diodes utilizing GaN tunnel junction. *Appl. Phys. Express* **2018**, *11*, 042101.
(26) Krishnamoorthy, S.; Akyol, F.; Akyol, S. InGaN/GaN tunnel junctions for hole injection in GaN light emitting diodes. *Appl. Phys. Lett.* **2014**, *105*, 141104.
(27) Ambacher, O.; Majewski, J.; Miskys, C.; Link, A.; Hermann, M.; Eickhoff, M.; Stutzmann, M.; Bernardini, F.; Fiorentini, V.; Tilak, V.; Schaff, B.; Eastman, L. F. Pyroelectric properties of Al(In)GaN/GaN hetero- and quantum well structrures. *J. Phys.: Condens. Matter* **2004**, *14*, 3399.
(28) Jain, S. C.; Willander, M.; Narayan, J.; Overstraeten, R. V. III-nitrides: Growth, characterization, and properties. *J. Appl. Phys.* **2000**, *87*, 9665.
(29) Reddy, P.; Bryan, I.; Bryan, Z.; Tweedie, J.; Washiyama, S.; Kirste, R.; Mita, S.; Collazo, R.; Sitar, Z. Charge neutrality levels, barrier heights, and band offsets at polar AlGaN. *Appl. Phys. Lett.* **2015**, *107*, 091603.
(30) Yan, L.; Zhang, Y. T.; Xu, H.; Li, L.; Jiang, J. Y.; Huang, Z.; Han, X.; Song, J. F.; Du, G. T. Influence of in-situ SiN_x mask on the quality of N-polar GaN films. *Mater. Sci. Semicond. Process.* **2017**, *59*, 35.
(31) Zheng, Z. Y.; Chen, Z. M.; Chen, Y. D.; Huang, S. J.; Fan, B. F.; Xian, Y. L.; Jia, W. Q.; Wu, Z. S.; Wang, G.; Jiang, H. Analysis and modeling of the experimentally observed anomalous mobility properties of periodically Si-delta-doped GaN layers. *Appl. Phys. Lett.* **2012**, *100*, 212102.
(32) Zheng, Z. Y.; Chen, Z. M.; Wu, H. L.; Chen, Y. D.; Huang, S. J.; Fan, B. F.; Xian, Y. L.; Wu, Z. S.; Wang, G.; Jiang, H. Effect of periodic Si-delta-doping on the evolution of yellow luminescence and stress in n-type GaN epilayers. *J. Cryst. Growth* **2014**, *387*, 52.
(33) Zhao, G. Y.; Adachi, M.; Ishikawa, H.; Egawa, T.; Umeno, M.; Jimbo, T. Growth of Si delta-doped GaN by metalorganic chemical-vapor deposition. *Appl. Phys. Lett.* **2000**, *77*, 2195.
(34) Xie, M. H.; Cheung, S. H.; Zheng, L. X.; Ng, Y. F.; Wu, H. S.; Ohtani, N.; Tong, S. Y. Step bunching of vicinal GaN (0001) surfaces during molecular beam epitaxy. *Phys. Rev. B: Condens. Matter Mater. Phys.* **2000**, *61*, 9883.
(35) Lochthofen, A.; Mertin, W.; Bacher, G.; Hoeppel, L.; Bader, S.; Off, S.; Hahn, B. Electrical investigation of V-defects in GaN using Kelvin probe and conductive atomic force microscopy. *Appl. Phys. Lett.* **2008**, *93*, 022107.
(36) Kaufmann, U.; Schlotter, P.; Obloh, H.; Köhler, K.; Maier, M. Hole conductivity and compensation in epitaxial GaN:Mg layers. *Phys. Rev. B: Condens. Matter Mater. Phys.* **2000**, *62*, 10867.
(37) Won, D. J.; Weng, X. J.; Redwing, J. M. Effect of indium surfactant on stress relaxation by V-defect formation in GaN epilayers grown by metalorganic chemical vapor deposition. *J. Appl. Phys.* **2010**, *108*, 093511.
(38) Romano, L. T.; Van de Walle, C. G.; Ager III, J. W.; Götz, W.; Kern, R. S. Effect of Si doping on strain, cracking, and microstructure in GaN thin films grown by metalorganic chemical vapor deposition. *J. Appl. Phys.* **2000**, *87*, 7745.
(39) Manning, I. C.; Weng, X.; Acord, J. D.; Fanton, M. A.; Snyder, D. W.; Redwing, J. M. Tensile stress generation and dislocation reduction in Si-doped $Al_xGa_{1-x}N$ films. *J. Appl. Phys.* **2009**, *106*, 023506.
(40) Moram, M. A.; Kappers, M. J.; Massabuau, F.; Oliver, R. A.; Humphreys, C. J. The effects of Si doping on dislocation movement and tensile stress in GaN films. *J. Appl. Phys.* **2011**, *109*, 073509.
(41) Yan, L.; Zhang, Y. T.; Han, X.; Deng, G. Q.; Li, P. C.; Yu, Y.; Chen, L.; Li, X. H.; Song, J. F. Polarization-induced hole doping in N-polar III-nitride LED grown by metalorganic chemical vapor deposition. *Appl. Phys. Lett.* **2018**, *112*, 182104.
(42) Liu, K.; AlQatari, F.; Sun, H.; Li, J.; Guo, W.; Li, X. Polarization properties of wurtzite III nitride indicate the principle of polarization engineering. *arXiv:1808.07211v4*, **2020**.
(43) Zhang, L.; Ding, K.; Yan, J. C.; Wang, J. X.; Zeng, Y. P.; Wei, T. B.; Li, Y. Y.; Sun, B. J.; Duan, R. F.; Li, J. M. Three-dimensional hole gas induced by polarization in (0001)-oriented metal-face III-nitride structure. *Appl. Phys. Lett.* **2010**, *97*, 062103.
(44) Choi, S.; Kim, J.; Kim, S. S.; Liu, J. P.; Kim, J.; Ryou, J. H.; Dupuis, R. D.; Fischer, A. M.; Ponce, F. A. Improvement of peak quantum efficiency and efficiency droop in III-nitride visible light-emitting diodes with an InAlN electron-blocking layer. *Appl. Phys. Lett.* **2010**, *96*, 221105.